16th World Conference on Earthquake, 16WCEE 2017
Santiago Chile, January 9th to 13th 2017
Paper N° 4946
Registration Code: S-B1464303322

APPLICATION OF MHVSR FOR SITE CHARACTERIZATION: STATE-OF-THE-ART

S. Molnar[1], J. F. Cassidy[2], S. Castellaro[3], C. Cornou[4], H. Crow[5], J. A. Hunter[6], S. Matsushima[7], F. J. Sánchez-Sesma[8], A. Yong[9]

[1] *Assistant Professor, University of Western Ontario, smolnar8@uwo.ca*
[2] *Earthquake Seismologist, Natural Resources Canada, john.cassidy@canada.ca*
[3] *Researcher, Università di Bologna, silvia.castellaro@unibo.it*
[4] *Professor, Université Grenoble Alpes, CNRS, IRD, IFSTTAR, USMB, cecile.cornou@ujf-grenoble.fr*
[5] *Geophysicist, Natural Resources Canada, heather.crow@canada.ca*
[6] *Emeritus Research Scientist, Natural Resources Canada, james.hunter@canada.ca*
[7] *Professor, Disaster Prevention Research Institute, Kyoto University, matsushima@sds.dpri.kyoto-u.ac.jp*
[8] *Professor, Universidad Nacional Autónoma de México, sesma@unam.mx*
[9] *Research Geophysicist, U.S. Geological Survey, yong@usgs.gov*

Abstract

Yutaka Nakamura (1989; [1]) popularized the application of the horizontal-to-vertical spectral ratio (HVSR) analysis of microtremor (ambient noise or vibration) recordings to estimate the predominant frequency and amplification factor of earthquake shaking. During the following quarter-century, popularity in the microtremor HVSR (MHVSR) method grew; studies have verified the stability of a site's MHVSR response over time and validated the MHVSR response with that of earthquake HVSR response. Today, MHVSR analysis is a popular reconnaissance tool used worldwide for seismic microzonation and earthquake site characterization in numerous regions, specifically, in the mapping of site period or fundamental frequency and inverted for shear-wave velocity depth profiles, respectively. However, the ubiquity of MHVSR analysis is predominantly a consequence of its ease in application rather than our full understanding of its theory. We present the state-of-the-art in MHVSR analyses in terms of the development of its theoretical basis, current state of practice, and we comment on its future for applications in earthquake site characterization.

Keywords: microtremor, HVSR, Nakamura method, guidelines, diffuse fields

1. Introduction

Ambient noise methods measure background seismic noise to assess the mechanical properties of the earth's subsurface, in particular seismic velocities. Ambient noise is defined as the constant vibration of the earth's surface, generated by the combination of low frequency (less than ~1 Hz) natural phenomena (earthquakes, wind, tides, rivers, rain, variations of atmospheric pressure) and high frequency (greater than ~1 Hz) human activities (road traffic, machinery, pedestrians). This background noise is a mixture of various wave types, which contain information on the sources and transmission paths of waves, and subsurface structure [2]. Most sources of ambient noise are located at the surface of the earth or at the bottom of the sea, releasing most of their energy as surface waves. Rayleigh waves become predominant at large distances because their geometric attenuation is much lower than that of body waves [3]. It is commonly assumed that Rayleigh and Love waves dominate an ambient noise record at more than one wavelength from the sources [4]. It is, however, impossible to isolate every wave from an ambient noise record. Aki [5] proposed to analyze ambient noise as a temporal and spatial stochastic process with reference to the nature of wave propagation. By recording the background noise over a long time period with an array of sensors, the record is considered an assemblage of coherent waves travelling in various directions over an extended frequency interval, which typically includes frequencies between 0.5 to 20 Hz.

This paper reviews the basis for the development of the single-station microtremor horizontal-to-vertical spectral ratio (MHVSR) method for retrieval and evaluation of the resonance frequencies of unconsolidated sediments over high velocity bedrock. We first review numerical and empirical studies that have examined composition of the microtremor wavefield (body and/or surface waves) in terms of a site's layered earth structure (e.g., complexity of layering, impedance contrast(s), and attenuation) and site response (e.g., resonance frequency and its lateral

variation). Recent developments on the theoretical basis of MHVSR response considering the microtremor wavefield as comprised of diffuse waves [6, 7] is also presented. Currently, MHVSR analysis varies amongst practitioners. We review published literature to document variations in equipment, data collection procedures, and processing methods from which to develop international recommendations of MVSR analysis for seismic site characterization [8, 9]. A short summary of studies that have led to the development of inversion and/or forward modelling techniques performed with MHVSR data is presented. We then present applications of MHVSR analyses including two detailed case studies.

In general, MHVSR analysis is currently applied to estimate the site period or fundamental frequency, and in certain circumstances, the site amplification factor, as observed in weak-motion (linear) earthquake shaking. The physics behind the MHVSR manifestation appears to be wavefield dependent (i.e., composed of body, surface, or diffuse waves and/or combinations thereof) [10] and therefore no single analytical expression exists as yet for all real-world conditions. Regardless, many practitioners also invert the MHVSR peak and/or its entire spectrum for models of subsurface shear-wave velocity structure or 1-D depth profiles [11, 12, 13, 14]. In other words, the physics-based forward-modeling codes for the inversion varies amongst practitioners, but the inversion of MHVSR is able to provide models of subsurface shear-wave velocity depth structure [12]. The uncertainty of these MHVSR-inverted velocity models may be improved further via joint inversion with dispersion data or by narrowing model parameter distribution bounds during the inversion based on supplemental geotechnical data.

2. MHVSR Development and Usage

The MHVSR method is an analysis technique that calculates the ratio of the horizontal-to-vertical Fourier spectra derived from microtremor (ambient noise or vibrations), typically recorded at a specific location by a three-component sensor. This single-station microtremor approach was initially developed in Japan by Nogoshi and Igarashi (1971) [15], based on studies by Kanai and Tanaka (1961) [16], for characterizing site response under seismic loading, and was later popularized and diffused by Nakamura [1] as reviewed in [17]. Early on, the MHVSR method gained notoriety and use in Europe (e.g., SESAME project; [8, 18]) and later in Canada [9, 19] and South America [20]. Its application in the United States, however, has not been as prolific.

2.1 Empirical development

Empirical evidence shows that the maximum of the MHVSR generally occurs at, or close to, the fundamental horizontal component of shear wave motion (SH) resonance frequency of the site (f_0), provided that there is a sufficiently strong impedance contrast at depth [21, 11, 22, 23, 24, 25, 26, 27, 28, 29,30]. Peak resonance amplification from one-dimensional (1D) vertical propagation of SH-waves through a single soil layer over a half-space occurs at

$$f_n = n(V_S/4h), \quad (1)$$

where V_S and h designate soil shear-wave velocity and thickness, respectively, and the index n (n =1, 3, 5, etc) designates the nth mode of oscillation [31]. Bonnefoy-Claudet et al. [32] demonstrated that this holds when microtremors are composed mostly of both body and/or surface waves. The microtremor H/V curves are diagnostic of key features of the subsurface structure. First, they indicate, through the peak amplitudes, whether stiff layers are present and, through the peak frequencies with an assumption of V_S (Eq. 1), depth of soil thickness and/or resonance, e.g., [11, 33, 34, 12]. Second, their variation in space or peculiar shape usually indicates lateral heterogeneities in the subsoil, e.g., [32, 35, 36, 37, 38, 39, 40, 41], and the interpretation of peak frequency and amplitude should be carefully considered for such sites. Third, they can show velocity reversals [13].

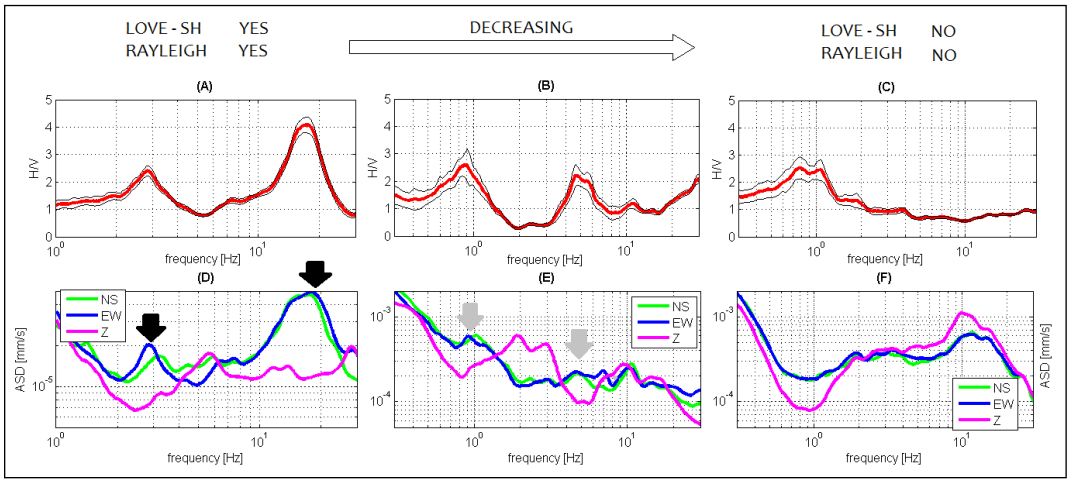

Figure 1. MHVSR (average ± standard deviation) curves at different sites (top) and single spectral components (NS, EW, Z) at the same sites (bottom). The contribution of Rayleigh waves is well visible at all sites (local minimum in the vertical component at f_0, local maximum at ~$2f_0$) in panels D, E and F. The contribution of Love-SH waves is marked by two distinct spectral peaks of the horizontal components at the two resonance frequencies in panel D (black arrows), by two modest peaks in panel E (grey arrows) while it is not present at all in panel F at f_0. From [12].

Studies of microtremors have demonstrated that the contribution of different surface wave types varies with frequency from site to site and that Love waves most often dominate the microtremor wavefield [42, 43, 44, 45]. However, the Rayleigh wave signature (local minimum of the vertical spectral component) (Figure 1) is always present, because surface waves attenuate less than body waves with distance from the source and they also have less stringent existence conditions compared to Love waves [12]. This ubiquitous feature allows to distinguish MHVSR peaks of stratigraphic origin from peaks of anthropic origin [13], whereas peaks of anthropic origin appear as narrow spikes in all three spectral components [12].

2.2 Theoretical development

Understanding the composition of microtremor is important, particularly to model the MHVSR curves in terms of *Vs* profiles. Over the years, different authors have attempted to explain the MHVSR phenomenology in terms of SH waves [1, 46], of Rayleigh waves [22, 26, 29, 47, 48] and by adding the effects of Love waves [49]. Recent studies are considering the role of all waves, the so called total field [6, 32, 50]. It was found that microtremor composition differs not only as a function of velocity and attenuation structure, but also as a function of the temporal and spatial distribution of the sources and their wave type and strength. The inversion of the MHVSR curve requires not only the knowledge of the specific sources acting at the site, but also several other soil parameters (e.g. Poisson's ratio, damping of each layer, 2D effects) that are often not easy to determine. This makes the MHVSR inversion an intrinsically imprecise process, but the lack of precision does not mean that the approach is useless or not important.

Sánchez-Sesma et al. [6] proposed that microtremors form a diffuse field containing all types of body (P and S) and surface waves (Love and Rayleigh) for which their associated illumination strengths stabilize in fixed proportions. Within the diffuse field assumption (DFA) multiple scattering and its equilibrating effects play a prominent role. The relative power of each seismic state that composes the illumination emerges from the principle of equipartition of energy. Theory asserts that within a diffuse elastic wave field the autocorrelation in the frequency domain (the power spectrum), at any point of the medium, is proportional to the imaginary part of the Green's function for source and receiver at the same point. As average autocorrelations are proportional to average directional energy densities (DED) then, by following [47] one way to assess the MHVSR is the square root of the ratio of the DEDs: $H/V=\sqrt{((E_1+E_2)/E_3)}$, where $E_\#$ are the DEDs for the horizontal (E_1 and E_2) and vertical (E_3) degrees of freedom. In other words, it is the square root of the ratio of the spectral averages of horizontal and vertical energies. The DFA allows linking measurements with intrinsic properties of system. The MHVSR is modeled in terms of Green's functions, where

$$H/V=\sqrt{((ImG_{11}+ImG_{22})/ImG_{33})}. \quad (2)$$

In Figure 2 the results of $ImG_{11}(0,0;\omega)$ and $ImG_{33}(0,0;\omega)$ for a single layer over a relatively rigid half-space are shown. The MHVSR computed using Eq. (2) is displayed with black lines.

For a horizontally layered medium this approach is straightforward for data at the surface [6, 7] and at depth [51]. Lateral heterogeneity can be dealt with similarly but computing Green's functions become computationally expensive [41]. In the case of layered media, the imaginary part of Green function is obtained as integrals in the horizontal wavenumber that can be computed using Bouchon's [52] discrete wavenumber method or alternatively, Cauchy's residue theory [53] that allows separate calculation of the contribution of the different parts of the elastic wave fields (body and/or surface waves). In this context, the inverse problem emerges; the target is to assess the soil elastic parameters from surface measurements. Diverse methods of gradient and heuristic types are useful for this purpose, and they all have advantages and limitations. Based on this formulation, García-Jerez et al. [54] developed a computer code for the efficient forward computation and inversion of MHVSR. The non-uniqueness issues, inherent in any inversion process, can be mitigated by performing joint inversion of H/V and dispersion curves [55]. In fact, the joint fit of H/V and dispersion curves was proposed by several authors, e.g., [56, 57, 58, 14, 59, 60, 61], and V_S profiles matching both the experimental MHVSR and dispersion curves are commonly considered better constrained than models based on the match of the curve from a single technique.

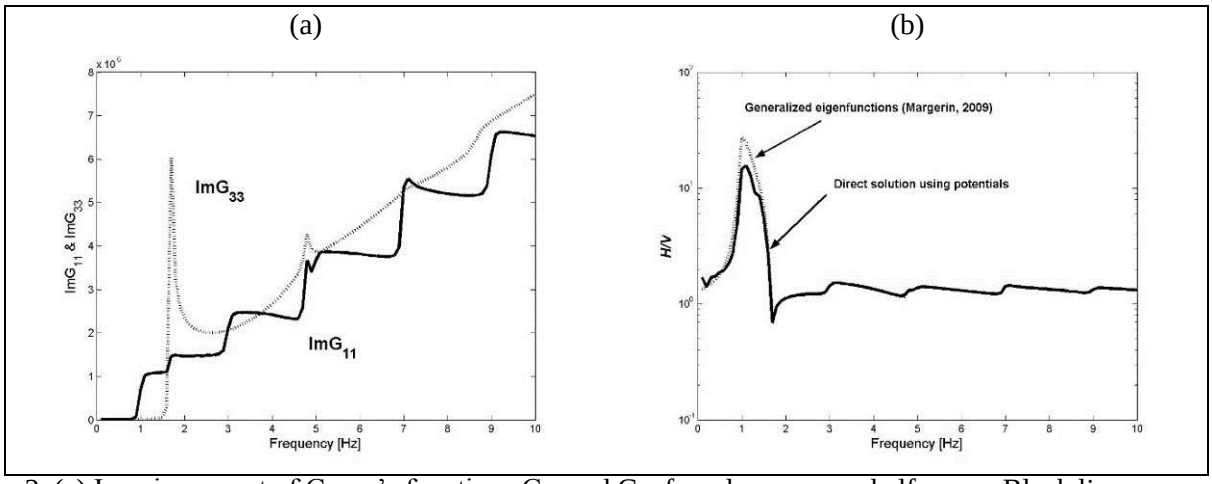

Figure 2. (a) Imaginary part of Green's functions G_{11} and G_{33} for a layer over a half space. Black line corresponds to horizontal response while dotted line represents vertical one. (b) MHVSR computed using Eq. (2).

Within the DFA it is possible to consider that the illumination is given only by body waves. Considering the scalar 1D problem, Claerbout [62] found that: "The reflection seismogram from a surface source and a surface receiver is one side of the autocorrelation of the seismogram from the source at depth and the same receiver." Kawase et al. [63] interpreted this observation as the 1D expression of the identity between autocorrelation and the imaginary part Green's function. Moreover, they developed criteria to apply the DFA for incoming body waves. Alternatively, the Rayleigh wave ellipticity can be extracted from microtremors by using multiple [64-66] or single-station [67] methods. The main advantage is no assumption of the microtremor sources is required. As for MHVSR, the joint inversion of ellipticity and dispersion curves [68] is advantageous for retrieving the horizontally layered V_S structure.

3. MHVSR Procedure

3.1 Field Data Collection

The most suitable recording instrument is a three-component seismometer (velocimeter) with a noise floor clearly lower than the ambient noise level over the frequency band of engineering interest (0.1-25 Hz). The natural frequency of the seismometer (digitizer included) should be considered with the estimated site conditions, i.e., depth to (rock) impedance interface. Accelerometers, with a relatively high intrinsic noise level, should generally

be avoided [69]. It is also recommended that the sampling rate shall be twice the frequency of engineering interest, e.g., 50 Hz for analysis of frequencies up to 25 Hz.

The seismometer is levelled on the earth's surface at a location of interest where the surface conditions should be representative of natural free-field ground characteristics. Coupling of the sensor to the earth's surface is crucial, hence, vegetation should be removed, feet inserted firmly into soft soil and protected from direct wind [70]. Sensor levelling or stability of the ground surface should be maintained throughout the recording duration. When there is variability in the MHVSR as a result of the surface ground conditions, the best practice is to either collect only on the "bare" ground surface (without man-made constructed materials) or acquire two or more recordings on different man-made surfaces in the immediate vicinity (within ~1 meter) to verify MHVSR redundancy.

Urban environments present significant challenges to the natural free-field ground condition. Measurements on very stiff artificial man-made material (e.g., pavement) over softer soils should be avoided as the peak of the MHVSR curve may be altered [13]. To circumvent this challenge and determine the variability of the signal, it is recommended that a number of repeated measurements be performed. It is, however, not recommended to perform this method over underground cavities (e.g., subways, tunnels). In a built downtown environment, any open parks or courtyards should be sought. Caution should be practiced, e.g., landscaping that overlies possible cavities or other buried man-made materials such as electrical power or vents, should be avoided. As a last resort, the user may perform measurements on the foundation floor of a man-made structure [8]. With regards to recording on or adjacent to man-made structures, the general rule of thumb is to offset the recording location by ~15 m from the structure [58]. Sustained vibrations from machinery will impact the MHVSR adversely when within the same frequency bandwidth of the location's fundamental frequency as single filtering techniques cannot remove these records; the measurement must be repeated when the machinery is not in operation.

The duration of data acquisition is defined by the targeted (bedrock) depth as well as quality of the ambient noise collected. The duration of recording must increase with depth of investigation. It is recommended that a minimum of 15-30 minutes of recording be performed to ensure sufficient time windows (statistics) are collected for the HVSR analysis – accounting for non-useable time segments (e.g., amplitude saturation) [8, 57, 71, 72].

One MHVSR analysis per site is sufficient to obtain an estimate of f_0, especially in conjunction with previous earthquake and MHVSR analyses, for confirmation of an expected pattern. At a previously unexplored site or where artifacts of man-made origin are expected, it is recommended to take multiple recordings at different times of the day or on different days to establish stability of the MHVSR curve. For microzonation studies, measurements should be obtained at a coarse or large spacing and reduced to a finer scale or denser spacing where rapid variations of the fundamental frequency are observed.

3.2 MHVSR Analysis

- The entire microtremor three-component time series is split into several time windows of equal or varying length. Window length is inversely proportional to minimum frequency – longer time windows should be used to measure stable low fundamental frequency sites.
- Fourier spectra are computed for every time window and smoothed.
- The ratio between horizontal and vertical spectra is then performed. As a first pass, the user shall compute ratios using each horizontal spectrum, rather than an average of the two horizontal spectra. Once it is confirmed that the two horizontal spectra are similar (indicative of underlying soil homogeneity), then the average HVSR is valid for use at this location. When the two horizontal spectra are not similar, the two HVSRs should be shown and considered individually in further analysis.
- The final average H/V ratio for the location was first calculated as the average of all H/V ratios from the spectra of each time window [1, 8, 15, 26], but is increasingly determined from the averaged spectra from all time windows of each component [6, 47, 50, 55].

Editing of the individual HVSRs from which to calculate an average shall be accomplished in the time or frequency domain. Transients (in time or frequency) may be removed manually or via an automatic algorithm.

3.3 Interpretation and Reporting

The calculated HVSR shall be interpreted in conjunction with the individual Fourier spectra (i.e., two plots are required, see Figures 1 and 2) to attribute observed peaks to natural free-field ground conditions and not sustained machinery vibrations. Peaks in the HVSR plots that are a consequence of natural underlying ground conditions exhibit an "eye-shape" in the Fourier spectra [13], in which horizontal spectra are of larger amplitude than the vertical spectrum over a limited bandwidth. In other words, HVSR peaks that result solely from a reduction in vertical spectrum amplitude are potentially not legitimate.

The frequency and amplitude level of each observed MHVSR peak, interpreted to be a consequence of natural ground conditions, is reported. To capture the shape of the MHVSR peak (narrow vs. broad), a measure of its frequency breadth is generally provided via fitting a standard normal or Gaussian function to the peak, e.g., [73], and reporting the required standard deviation or reporting the range in frequency at the mid-height of the peak.

Amplitude of MHVSR peaks are not used directly to estimate earthquake site amplification factors. Many studies have shown lower MHVSR amplitudes than found in earthquake HVSR (EHVSR) peaks ([25] lists 18 studies). Conversely, similar agreement between MHVSR and EHVSR has been demonstrated at strong impedance contrast sites, e.g., [19]. As shown from numerical [39, 74] and empirical [75] studies, the amplitude of MHVSR peaks scales with the impedance contrast, which is useful to qualify the impedance contrasts of layered earth models.

4. Applications and Case Studies

MHVSR studies are becoming increasingly popular around the world, resulting in a growing number of articles documenting the importance and robustness of MHVSR results. For example, demonstrating agreement between results from MHVSR studies with those from other geophysical techniques and geological observations [28, 33, 76-79]. MHVSR studies are particularly valuable in low-seismicity regions where detailed fundamental site-period maps can be generated and used for urban planning purposes, e.g., [37, 60, 76, 80, 81]. MHVSR studies have been applied for liquefaction hazard mapping, e.g., [82, 83], and for engineering applications such as evaluating both building and soil response using ambient noise, e.g., [58, 84-88]. Combining techniques, such as MHVSR and Multi-channel Analysis of Surface Waves (MASW), e.g., [89] or ambient vibration array, e.g., [60], is particularly beneficial at evaluating earthquake site response in areas of low seismicity and has also been used (MHVSR and cross-correlation of ambient seismic noise) to characterise deep basin structure, e.g., [90].

4.1 Seismic Site Characterization Using MHVSR and Noninvasive Multi-methods in the U.S.

Before the ARRA-funded (American Recovery and Reinvestment Act) site characterization project [91], MHVSR analyses were not commonly applied in the U.S. despite its popularity elsewhere. The Yong et al. (2013; [91]) (henceforth: Y13) project had two objectives: (1) to acquire a range of site-specific geophysical data for the ground motion modeling community, and (2) to establish a pilot project for the Advanced National Seismic System (ANSS; http://earthquake.usgs.gov/monitoring/anss/; last accessed 11 May 2016) to guide similar efforts in the future. The most important task in the project was the determination of V_{S30}, the time-averaged shear-wave velocity (V_S) from the surface to the depth of 30 meters. A total of 191 strong-motion station sites were characterized; 187 sites are in California and four in the Central-Eastern United States, to demonstrate that noninvasive methods could be used outside of California. Only about half (51%) of the sites have V_{S30} based on collocated measurements recorded by multiple methods. Nevertheless, microtremor data were specifically recorded at all 191 sites for MHVSR analysis. The Y13 report [91], along with site and raw data, are available online at http://pubs.usgs.gov/of/2013/1102/ (last accessed 11 May 2016).

The Y13 project typically made MHVSR measurements at three locations of each array for two main purposes: to demonstrate whether or not modeling the subsurface velocity structure as 1D is appropriate and to estimate the f_0 of the site [8]. The MHVSR measurement locations are generally distributed at the end- and mid-points of each survey array segment. Frequently, one of the MHVSR records was obtained adjacent to the ANSS station. The primary seismic system used to acquire MHVSR data was a Nanometrics Trillium Compact 120 s seismometer and a Kinemetrics Quanterra Q330 data recorder. MHVSR measurements were also made at some sites with a Micromed (now Moho s.r.l) Tromino ENGY. The data acquisition procedures generally followed user guidelines developed under the SESAME [8, 18] project. The Trillium Compact was primarily deployed in a shallow hole

(Figure 3a), coupled to the ground by a small aluminum cradle with spikes, covered with a plastic tub to isolate the effects of wind (Figure 3b). In gravelly soil, the aluminum cradle was coupled to the ground using gypsum plaster. Microtremor data were recorded at a 200 Hz sampling rate. Relative to the Trillium Compact, the Tromino is a higher frequency standalone seismic system (seismometer and data recorder combined) optimally designed for MHVSR measurements. Y13 typically only used Trominos at sites that were expected to have relatively shallow depth to bedrock. The duration of microtremor measurements were typically between 15 and 45 minutes, depending on site conditions, and data were recorded at 128 samples per second. Recordings were stored in the instrument's internal memory and downloaded to a laptop computer for viewing in the software package (Grilla version 6.1) provided by the manufacturer.

The Geopsy software package (version 2.7.0) (*http://www.geopsy.org*; last accessed 11 May 2016) was used for MHVSR analysis. MHVSR was typically calculated over a frequency range dependent on the observed site response and using a time window length of 100–200 s. Time windows containing transients (nearby pedestrian or vehicular traffic) or segments yielding poor quality results were not utilized for analysis. For every selected time window, Fourier amplitude spectra were calculated and smoothed by applying the Konno and Ohmachi [92] filter with a smoothing coefficient value between 30 and 40. The vertical amplitude spectra were divided by the root-mean-square (RMS) of the horizontal amplitude spectra to calculate the MHVSR for each time window and the average MHVSR. After calculating the standard deviation of the MHVSR amplitudes for all windows, the average response is divided and multiplied by the standard deviation to produce the minimum and maximum MHVSR spectra, respectively [8]. MHVSR data were not typically modeled and no attempt was made to jointly invert MHVSR and surface-wave dispersion data. Occasionally, primarily at shallow rock sites, MHVSR modeling routines available in software packages (Grilla [Moho s.r.l.] and Seisimager [Geometrics/Oyo Corporation]) were used to calculate the theoretical MHVSR response for the V_S models developed by the inversion of the surface-wave dispersion data, and then these responses were compared to the measured MHVSR data.

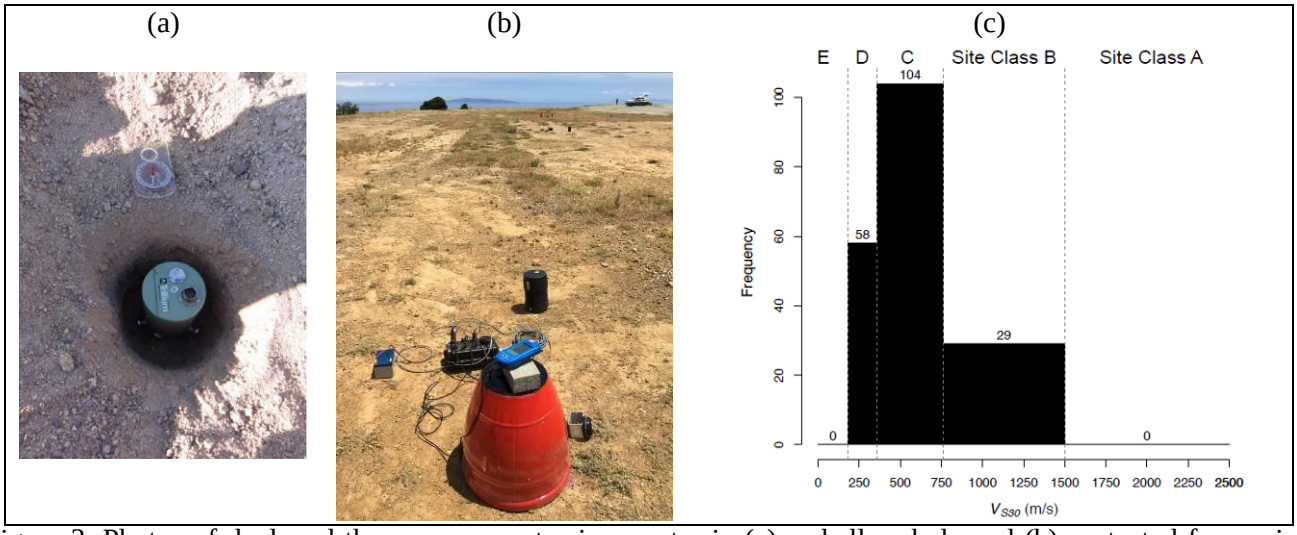

Figure 3. Photos of deployed three-component seismometer in (a) a shallow hole and (b) protected from wind (seismometer under red tub with RefTek 130S Data Acquisition System) [91]. (c) Distribution of V_{S30} amongst the 191 tested sites [91].

At the end of the Y13 project, V_S profiles and V_{S30} estimates were produced for 187 stations in California and four in the CEUS. These results represent a significant increase (approximately doubling) in the number of measurement-based V_{S30} values for strong motion stations in California [93, 94]. As a pilot project, the experience provided the ANSS with information necessary to begin evaluating measurement techniques and to develop guidelines for characterizing seismic site conditions at other strong motion stations. Studies about the Y13 calculated MHVSRs with respect to the expected site 1D responses are currently ongoing, thus their results are expected to play a key role in determining the reliability of the V_S profiles and V_{S30} derived from surface-wave methods.

4.2 Fundamental Site Period Studies in Canada's National Capital Region – the Soft Sediment Case

The highly populated St Lawrence Lowlands, stretching from Ottawa, Ontario to Quebec City, Quebec, is a region characterized by zones of elevated seismic hazard. Near surface glaciomarine sediments (clayey silts and silty clays), present throughout the region in thicknesses up to 180 m, typically exhibit low V_S (< 180 m/s) and overlie high velocity tills and bedrock. Weak motion events recorded at soil and bedrock seismograph stations in the Ottawa area indicate soil-to-rock spectral amplification ratios can exceed 80 at the site fundamental frequency or period [75, 95, 96].

Early Geological Survey of Canada (GSC) studies of site resonance were conducted in a region east of Ottawa [97]. Intensive geological and geophysical studies were undertaken in the area to investigate heavily disturbed glaciomarine sediments interpreted to have resulted from paleoearthquake activity ca. 7060 years BP [98, 99]. At 40 test sites, fundamental periods were estimated from one-dimensional models using V_S measurements, and compared to H/V spectral ratios calculated from 60 min microtremor recordings using a Guralp (CGM-40T) seismometer. Results from both techniques indicated sharp, high amplitude, resonance peaks, but 1D models produced periods which were often higher than those calculated with the H/V method.

In 2006, the GSC undertook a multi-year demonstration study in Canada's national capital region (NCR) to systematically map the distribution of fundamental site periods (T_o) and seismic site categories (classes A through E) as defined in the 2005 National Building Code of Canada (NBCC). The joint cities of Ottawa and Gatineau, which define the NCR, are subject to seismic activity originating from the West Quebec Seismic Zone, and have been identified as having the third highest earthquake risk in Canada. The maps were compiled using subsurface geology derived from a database of 21,800 boreholes, and V_S data acquired at 750 reflection/refraction test sites, 25 km of high-resolution seismic landstreamer data, and nine downhole V_s logs [9, 75, 95, 100]. Both T_0 and seismic site class maps have a borehole database at their core, and were compiled by developing a well constrained average V_S-depth function derived from shear wave reflection surveys in soft glaciomarine sediments (Vs_{av}=123.86+0.88h ± 20.3 m/s), and establishing V_s ranges for glacial deposits (till) and bedrock using refraction survey results. These relationships allowed for each borehole record to be converted into a V_S profile, whereby V_{S30} could be determined for each borehole site. Results indicated that seismic site classes ranged from A to E and could rapidly change over short distances as bedrock depth varied in fault-controlled basins. Site class F, although present, could not be confirmed using geophysical methods alone and required site specific geotechnical testing. T_o were calculated using the quarter wavelength method [101], also called the equivalent single-layer (ESL) method, as outlined in the NBCC (editions 2005, 2010, 2015). As this approach is not constrained by a depth limitation of 30 m, T_0 were found to range from 0.0 seconds at outcropping bedrock, to 2.0 seconds where soft sediment reached 110 m in deep bedrock basins.

Since 2007, a Tromino seismograph (MoHo s.r.l.) has been used to record ambient noise at over 400 sites in the NCR, where 283 coincide with seismic test sites. At each microtremor site, data were recorded for a minimum of 30 minutes at 128 Hz sampling rate and processed using the Grilla software following the SESAME criteria [8]; 60-s time windows were used and frequency spectra calculated over 0.1-20 Hz using the Konno and Omachi [91] (b=40) filter. A cross plot of fundamental periods calculated using the two techniques (ESL and HVSR) are presented in Figure 4. As observed earlier in eastern Ontario [102], Figure 4a demonstrates that T_0 systematically deviate in this geological setting, reaching 30% at 2.0 s. This deviation, which has been quantified by a power function, is attributed to the effects of significant V_S gradients in the glaciomarine sediments (the "Dobry effect", [103]) which are not taken into account with the ESL approach. By applying a multilayer soil model, Motazedian et al. [104] found that T_o is reduced when compared to the ESL approach. By using the Dobry velocity gradient-versus-depth correction following the Hadijan [105] approach, Motazedian et al. [15] were able to closely model the observed curve given in Figure 4b.

The influence of 2D and 3D bedrock topography on HVSR period (or frequency), and peak amplitude and shape was further investigated using high resolution seismic reflection profiles throughout the study area. Figure 5 presents a shear wave seismic section collected with a landstreamer array over a bedrock basin, up to 120 m deep, filled with soft glaciomarine sediments [106]. Seven HVSR profiles are displayed at sites along the section, showing variation in shape as sediment thickness and bedrock slope change along the alignment. These, and an additional 82 individual MHVSRs (with depth-control provided by boreholes or seismic profiles), were used to

create a site-specific frequency-depth curve presented in Figure 4b. This curve was used to identify the shape of a 3 km by 1 km bedrock basin, which was instrumented in 2010 with an array of one bedrock and five soil seismograph stations to monitor basin response during earthquake shaking. To address the impact of 3D resonator topography on HVSR curve shape, the authors suggest that the horizontal resolution of the resonator surface using the MHVSR technique could be guided by the Fresnel Zone radius, as determined by the fundamental site frequency.

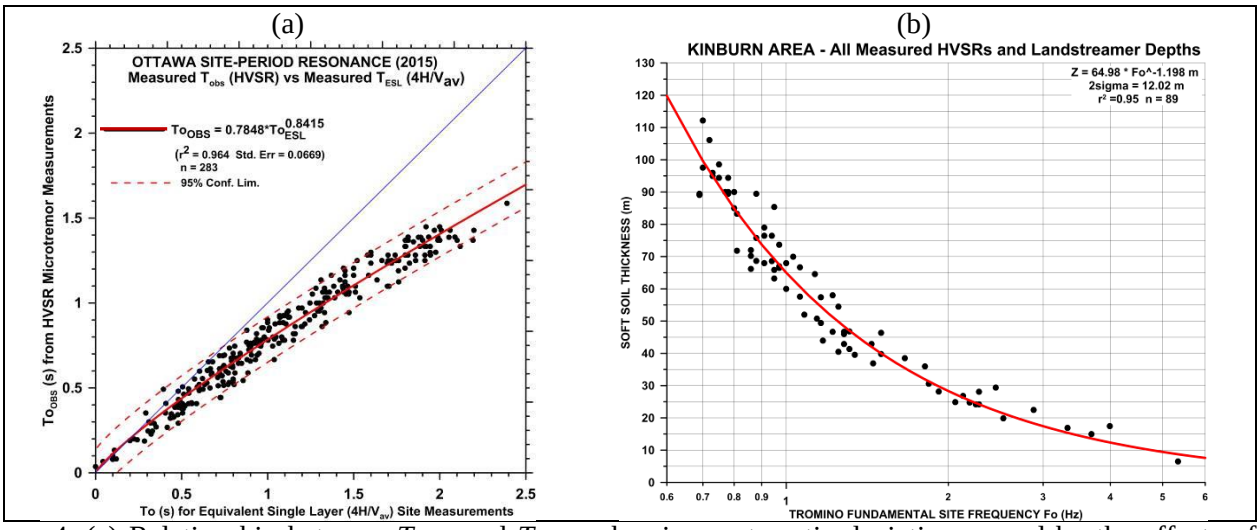

Figure 4. (a) Relationship between T_{0ESL} and T_{0HVSR} showing systematic deviation caused by the effects of V_S gradients in the soft glaciomarine sediments. (b) Sample site-specific relationship developed between T_{0HVSR} and the depth to the main impedance contrast using high resolution V_S reflection profiling. Our experience leads us to recommend converting fundamental periods from microtremor measurements to sediment thicknesses only for well-studied sites where subsurface structure and velocities are well understood.

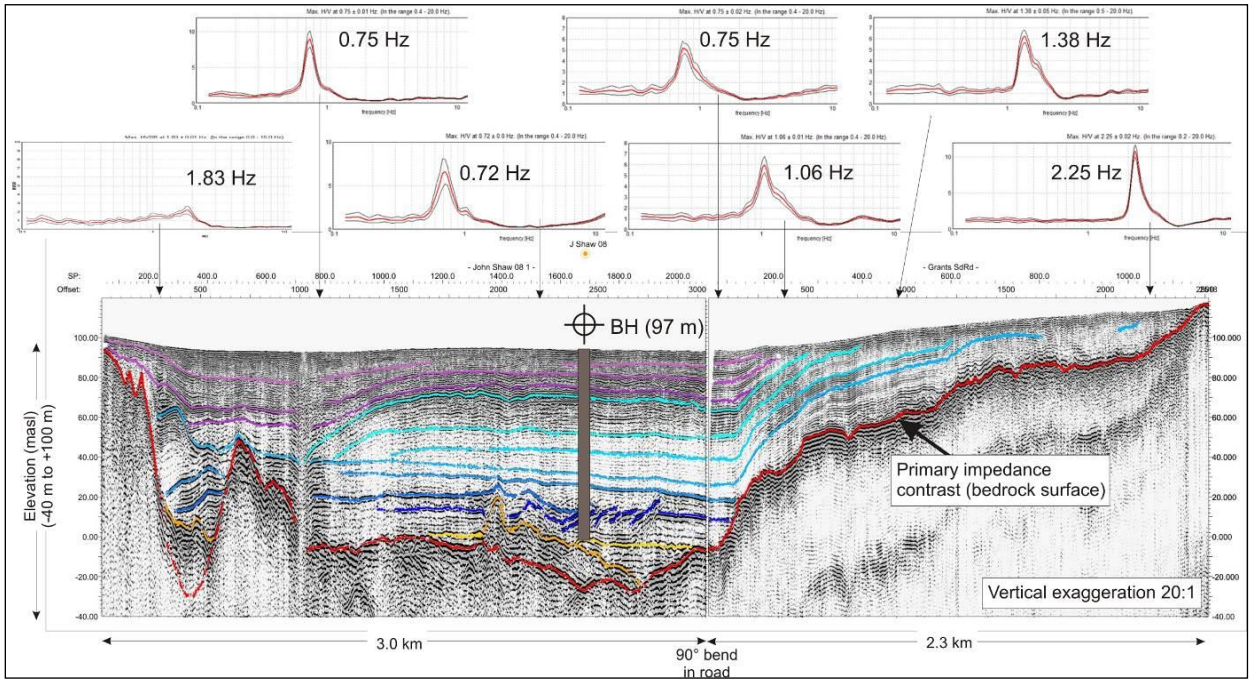

Figure 5. High resolution shear wave velocity profiles collected near Ottawa, Ontario, showing a bedrock basin containing sand and gravel eskers (yellow and orange horizons) at its base, overlaid with glaciomarine clayey-silt sediments (blue and purple horizons). A 97 m, continuously cored, borehole was PVC-cased for geophysical logging. Seven sample HVSR profiles collected along the seismic lines are presented to demonstrate the influence of sediment thickness and bedrock slope on peak frequency, amplitude, and sharpness within a homogenous sediment setting (seismic section adapted from [106]).

5. Concluding Remarks

During the last two decades, we have seen substantial progress in development of the single-station MHVSR analysis approach, or "the Nakamura method" [1]. Its use is prevalent in seismic microzonation mapping, post-earthquake reconnaissance, and earthquake site characterization in particular, including MHVSR peak frequency for soil thickness and MHVSR inversion for V_S depth structure. Its practical ease and small volume of equipment, thereby minimal expense, has resulted in truly global applications, notably including Africa [107] and Antarctica [108].

This paper reviewed the original basis for the development of the MHVSR method including numerical and empirical studies that have examined composition of the microtremor wavefield. Recent developments on the theoretical basis of MHVSR response are presented that consider the microtremor wavefield as comprised of diffuse waves [6, 7]. MHVSR analysis varies amongst practitioners, thus, published literature is reviewed to document variations in equipment, data collection and processing methods from which to develop international recommendations of MVSR analysis for seismic site characterization [8, 9]. Short summaries of studies that have led to the development of forward modelling and/or inversion techniques performed with MHVSR data were also presented. In addition, applications of MHVSR analyses are presented from two detailed case studies in North America.

As the uses of MHVSR and other noninvasive surface-wave based methods become more prolific, groups of key developers and practitioners of the noninvasive methods have recently began to gather to discuss the state of knowledge and practice in surface wave based methods with the motivation to establish best-practices and guidelines for applying noninvasive geophysical site characterization methods [9, 109, 110]). Following from previous guideline projects [8, 9], the authors of this paper (amongst others) have initiated the next stages in development of the MHVSR analysis method and other noninvasive methods by establishing an international consortium to develop the "COSMOS International Guidelines for the Application of Noninvasive Geophysical Techniques to Characterize Seismic Site Conditions" (http://www.cosmos-eq.org/COSMOS_Newsletter_22.pdf; last accessed 31 May 2016).

6. Acknowledgements

Any opinions, findings, and conclusions or recommendations expressed in this material are those of the authors and do not necessarily reflect the views of the Consortium of Organizations for Strong-Motion Observation Systems (COSMOS) Facilitation Committee for the Development of the COSMOS International Guidelines for the Application of NonInvasive Geophysical Techniques to Characterize Seismic Site Conditions.

Any use of trade, firm, or product names is for descriptive purposes only and does not imply endorsement by the U.S. Government.

Thanks are given to J Piña-Flores for his comments and suggestions. To G Sánchez, E Plata and their team of the Unidad de Servicios de Información (USI) of the Institute of Engineering-UNAM for locating useful references. Partial support by AXA Research Fund, by DGAPA-UNAM under Project IN104712 is gratefully acknowledged.

Natural Resources Canada (Geological Survey of Canada) gratefully acknowledges the support of the Public Safety Geoscience and Groundwater Geoscience Programs. This is ESS Contribution number 20160175.

This paper was improved from U.S. Geological Survey reviews by Drs. Stephen Hartzell and William Stephenson.

7. References

[1] Nakamura, Y. (1989). A method for dynamic characteristics estimation of subsurface using microtremors on the ground surface, Quarterly Report of Railway Technical Research Institute (RTRI), 30, 25-33.

[2] Okada, H., 2003, The Microtremor Survey Method, Geophysical Monograph Series Number 12: Tulsa, Oklahoma, Society of Exploration Geophysicists, 135 p.

[3] Socco, L. V., C. Strobbia. (2004). Surface Wave Methods for near-surface characterisation, a tutorial: Near Surface Geophysics, 2, 165–185.

[4] Arai, H. & K. Tokimatsu (2005). S-Wave Velocity Profiling by Joint Inversion of Microtremor Dispersion Curve and Horizontal-to-Vertical (H/V) Spectrum, Bull. Seismol. Soc. Am. 95, 1766-1778.

[5] Aki K (1957). Space and time spectra of stationary stochastic waves, with special reference to microtremors, Bull. Earthq. Res. Inst., 35, 415-456.
[6] Sánchez-Sesma F J, Rodríguez M, Iturrarán-Viveros U, et al. (2011). A theory for microtremor H/V spectral ratio: application for a layered medium. Geophysical Journal International 186(1), 221-225.
[7] Kawase, H., S. Matsushima, T. Satoh, and FJ Sánchez-Sesma (2015). Applicability of theoretical horizontal-to-vertical ratio of microtremors based on the diffuse field concept to previously observed data, BSSA, 106.
[8] SESAME (2004). Guidelines for the implementation of the H/V spectral ratio technique on ambient vibrations: Measurements, processing, and interpretation, SESAME European research project, WP12 – Deliverable D23.12.
[9] Hunter, J.A. and Crow, H.L. (ed.), 2012. Shear Wave Velocity Measurement Guidelines for Canadian Seismic Site Characterization in Soil and Rock; Geological Survey of Canada, Open File 7078, 227 p., doi:10.4095/291753.
[10] Lachet, C., and P.-Y. Bard (1994). Numerical and theoretical investigations on the possibilities and limitations of Nakamura's technique, Journal of the Physical Earth, 42, 377-397.
[11] Ibs-von Seht, M, J Wohlenberg (1999). Microtremor measurements used to map thickness of soft sediments. BSSA, 89, 250–259.
[12] Castellaro, S. (2016). The complementarity of H/V and dispersion curves, Geophysics, 81, 6, T323–T338.
[13] Castellaro S and Mulargia F (2009). The effect of velocity inversions on H/V, Pure Appl. Geophys., 166, 567–92.
[14] Castellaro S., Mulargia F., (2014). Simplified seismic soil classification: the VfZ matrix, Bull. Eq. Eng., 12, 735–754.
[15] Nogoshi, M., and T. Igarashi (1971). On the amplitude characteristics of microtremor (part 2), Journal Seismological Society of Japan, 24, 26–40.
[16] Kanai, K. and Tanaka T., 1961, On Microtremor VIII, Bull.Earthq. Res. Inst., Tokyo University, Vol.39, pp.97-114.
[17] Bonnefoy-Claudet, S., F. Cotton, and P.-Y. Bard (2006). The nature of noise wavefield and its applications for site effects studies: A literature review, Earth-Science Reviews, 79(3), 205–227.
[18] Bard, P.-Y., and SESAME participants, 2004. The SESAME project: An overview and main results, in Proceedings, 13th World Conference on Earthquake Engineering, Vancouver, August 2004, Paper #2207.
[19] Molnar, S., and JF Cassidy (2006). A comparison of site response techniques using weak-motion earthquakes and microtremors, Earthquake Spectra, 22, 169-188.
[20] Pilz M, Parolai S, Leyton F, Campos J, Zschau J (2009): A comparison of site response techniques using earthquake data and ambient seismic noise analysis in the large urban areas of Santiago de Chile. GJI 178, 713–728.
[21] Field & Jacob (1993). The theoretical response of sedimentary layers to ambient seismic noise, GRL, 20, 2925-2928.
[22] Lermo, J and FJ Chavez-Garcia (1994). Are microtremors useful in site response evaluation, BSSA, 84, 1350-1364.
[23] Bonilla, L. F., J. H. Steidl, G. T. Lindley, et al. (1997). Site amplification in the San Fernando Valley, California: Variability of site-effect estimation using the S-wave, Coda, and H/V methods, BSSA, 87, 710-730.
[24] Bour, M., Fouissac, D., Dominique, P. & Martin, C., 1998. On the use of microtremor recordings in seismic microzonation, Soil. Dyn. Earthq. Eng., 17, 465–474.
[25] Bard, P.-Y., 1999. Microtremor measurements: A tool for site effect estimation? Proceedings, 2nd International Symposium on the Effects of Surface Geology on Seismic Motion, Yokohama, December 1998, pp. 1251–1279.
[26] Fäh, D., F. Kind, D. Giardini (2001). A theoretical investigation of average H/V ratios, Geophys. J. Int., 145, 535-549.
[27] Woolery, E.W. and Street, R., 2002. 3D near-surface soil response from H/V ambient-noise ratios; Soil Dynamics and Earthquake Engineering, v. 22, p. 865-876.
[28] Parolai, S, P Bormann, and C Milkereit (2002). New relationships between Vs, thickness of sediments, and resonance frequency calculated by the H/V ratio of seismic noise for the Cologne area (Germany). BSSA, 92, 2521–2527.
[29] Malischewsky, P. G., and F. Scherbaum (2004). Love's formula and H/V-ratio (ellipticity) of Rayleigh waves, Wave Motion, 40, 57-67.
[30] Haghshenas, E., P-Y Bard, N Theodulidis, SESAME WP04 team, (2008). Empirical evaluation of microtremor H/V spectral ratio, Bull Earthquake Eng, 6, 75-108.
[31] Haskell NA, 1960. Crustal reflection of plane SH waves, J. Geophys. Res., 65, 4147-4150.
[32] Bonnefoy-Claudet S, S Baize, LF Bonilla, C Berge-Thierry, C Pasten, J Campos, P Volant, R Verdugo (2008). Site effect evaluation in the basin of Santiago de Chile using ambient noise measurements, GJI.
[33] Hinzen, K-G, B Weber, F Scherbaum (2004). On the resolution of H/V measurements to determine sediment thickness, a case study across a normal fault in the Lower Rhine Embayment, Germany. J. Earthquake Eng., 8, 909–926.
[34] Gosar, A, A Lenart (2010). Mapping the thickness of sediments in the Ljubljana Moor basin (Slovenia) using microtremors. Bulletin of Earthquake Engineering, 8(3), 501–518.
[35] Uebayashi, H. (2003). Extrapolation of irregular subsurface structures using the horizontal-to-vertical spectral ratio of long-period microtremors, Bull. Seism. Soc. Am., Vol. 93, 570-582.
[36] Roten, D., D. Faeh, C. Cornou, and D. Giardini (2006). Two-dimensional resonances in Alpine valleys identified from ambient vibration wavefields. Geophysical Journal International, 165(3), 889–905.
[37] Guéguen, P., C. Cornou, S. Garambois, and J. Banton (2007). On the limitation of the H/V spectral ratio using seismic noise as an exploration tool: application to the Grenoble valley (France), a small apex ratio basin, PaAG, 164, 115–134.
[38] Özalaybey, S, E Zor, S Ergintav, M C Tapırdamaz (2011). Investigation of 3-D basin structures in the Izmit Bay area (Turkey) by single-station microtremor and gravimetric methods. Geophysical Journal International, 186(2), 883–894.
[39] Uebayashi, Kawabe, Kamae (2012). Reproduction of microseism H/V spectral features using a three-dimensional complex topographical model of the sediment-bedrock interface in the Osaka sedimentary basin, GJI, 189, 1060–1074.
[40] Le Roux, O, C Cornou, D Jongmans, S Schwartz (2012). 1-D and 2-D resonances in an Alpine valley identified from ambient noise measurements and 3-D modelling. Geophysical Journal International, 191(2), 579–590.

[41] Matsushima, Hirokawa, De Martin, Kawase, Sánchez-Sesma (2014): The Effect of Lateral Heterogeneity on Horizontal-to-Vertical Spectral Ratio of Microtremors Inferred from Observation and Synthetics, BSSA, 104, 381-393.
[42] Arai, H. & K. Tokimatsu (1998). Evaluation of local site effects based on microtremor H/V spectra. Proceeding of the Second International Symposium on the Effects of Surface Geology on Seismic Motion. pp. 673–680.
[43] Yamamoto, H (2000). Estimation of shallow S-wave velocity structures from phase velocities of Love-and Rayleigh-waves in microtremors. Proceedings of the 12th World Conference on Earthquake Engineering.
[44] Köhler, A, M Ohrnberger, F Scherbaum, M Wathelet, and C Cornou (2007). Assessing the reliability of the modified three component spatial autocorrelation technique. Geophysical Journal International, 168(2), 779–796.
[45] Endrun, B. (2011). Love wave contribution to the ambient vibration H/V amplitude peak observed with array measurements. Journal of seismology, 15(3), 443–472.
[46] M. Herak (2008). ModelHVSR - A Matlab® Tool to Model Horizontal-to-Vertical Spectral Ratio of Ambient Noise, Computers & Geosciences 34, 1514–1526.
[47] Arai & Tokimatsu (2004). S-wave velocity profiling by inversion of microtremor H/V spectrum. BSSA 94, 53-63.
[48] Tuan, TT, F Scherbaum, PG Malischewsky (2011). On the relationship of peaks and troughs of ellipticity (H/V) of Rayleigh wves and the transmission response of single layer over half-space models, GJI, 184, 793-800.
[49] Van der Baan, M. (2009). The origin of SH-wave resonance frequencies in sedimentary layers, GJI, 178, 1587-1596.
[50] Lunedei, E., D. Albarello (2015). Horizontal-to-vertical spectral ratios from a full-wavefield model of ambient vibrations generated by a distribution of spatially correlated surface sources, Geophys. J. Int., 201, 1140–1153.
[51] Lontsi, AM, FJ Sánchez-Sesma, JC Molina-Villegas, M Ohrnberger, F. Kruger (2015). Full microtremor H/V(z, f) inversion for shallow subsurface characterization, GJI, 202, 298-312.
[52] Bouchon, M. (2003). A Review of the Discrete Wavenumber Method, Pure Appl. Geophys. 160 445–465.
[53] García-Jere, Luzón, Sánchez-Sesma, et al. (2013). Diffuse elastic wavefield within a simple crustal model. Some consequences for low and high frequencies. J. Geophys. Res., Solid Earth 118, 5577-5595.
[54] García-Jerez A, Piña-Flores J, Sánchez-Sesma F J, Luzón F, Perton M (in press). A computer code for forward computation and inversion of the H/V spectral ratio under the diffuse field assumption. Computers & Geosciences.
[55] Piña-Flores J, Perton M, García-Jerez A, Carmona E, Luzón F, Molina-Villegas JC, Sánchez-Sesma F J (submitted). The inversion of spectral ratio H/V in a layered system using the Diffuse Field Assumption (DFA). GJI.
[56] Parolai, S., M Picozzi, SM Richwalski, C Milkereit (2005). Joint inversion of phase velocity dispersion and H/V ratio curves from seismic noise recordings using a genetic algorithm, considering higher modes. GRL, 32, 1, L01303.
[57] Picozzi, M, S Parolai, D Albarello (2005). Statistical analysis of noise horizontal-to-vertical spectral ratios (HVSR). BSSA, 95, 1779–1786.
[58] Castellaro S and F Mulargia (2010). How Far from a Building Does the Ground-Motion Free-Field Start? The Cases of Three Famous Towers and a Modern Building, Bull. Seism. Soc. Am., 100, 2080-2094.
[59] Rošer, J, A Gosar (2010). Determination of V_{S30} for seismic ground classification in the Ljubjana area, Slovenia, Acta Geotechnica Slovenica, 61-76.
[60] Zor, Özalaybey, Karaaslan, et al. (2010). Shear wave velocity structure of the Izmit Bay area (Turkey) estimated from active–passive array surface wave and single-station microtremor methods. GJI, 182, 1603–1618.
[61] Foti, S, S Parolai, P Bergamo, G Di Giulio, M Maraschini, G Milana, M Picozzi, R Puglia (2011). Surface wave surveys for seismic site characterization of accelerometric stations in ITACA, Bull Earthquake Eng, 9, 1797-1820.
[62] Claerbout J (1968). Synthesis of a layered medium from its acoustic transmission response, Geophysics, 33, 2, 264-269.
[63] Kawase H, FJ Sánchez-Sesma, S. Matsushima (2011). Application of the H/V spectral ratios for earthquake and microtremor ground motions, Proceedings 4th IASPEI/IAEE International Symposium, ESG, U. Cali. Santa Barbara.
[64] Poggi, V. & Fäh, D., 2010. Estimating Rayleigh wave particle motion from three-component array analysis of ambient vibrations, Geophys. J. Int., 180, 251–267.
[65] Poggi, V., Fäh, D., Burjanek, J. & Giardini, D., 2012. The use of Rayleigh wave ellipticity for site-specific hazard assessment and microzonation: application to the city of Lucerne, Switzerland, Geophys. J. Int., 188, 1154–1172.
[66] Maranò, S., Reller, C., Loeliger, H.-A. & Fäh, D., 2012. Seismic waves estimation and wavefield decomposition: application to ambient vibrations, Geophys. J. Int., 191(1), 175–188.
[67] Hobiger, M., Bard, P.-Y., Cornou, C. & Le Bihan, N., 2009. Single station determination of Rayleigh wave ellipticity by using the random decrement technique (RayDec), Geophys. Res. Lett., 36, L14303, doi:10.1029/2009GL038863.
[68] Hobiger, M, C Cornou, M Wathelet, et al. (2013). Ground structure imaging by inversions of Rayleigh wave ellipticity: sensitivity analysis and application to European strong-motion sites. GJI, 192(1), 207–229.
[69] Guillier B., K. Atakan, J.-L. Chatelain, et al. and the SESAME Team, (2007). Influence of instruments on the H/V spectral ratios of ambient vibrations, Bull. Eq. Eng., doi: 10.1007/s10518-007-9039-0.
[70] Chatelain, J.-L., B. Guillier, F. Cara, A.-M. Duval, K. Atakan, P.-Y. Bard, et al. (2008). Evaluation of the influence of experimental conditions on H/V results from ambient noise recordings. Bull. Earthquake Eng., 6(1), 33–74.
[71] Parolai, S and JJ Galiana-Merino (2006). Effect of transient seismic noise on estimates of H/V spectral ratios. BSSA, 96(1), 228–236.
[72] Albarello, D. and E. Lunedei (2013). Combining horizontal ambient vibration components for H/V spectral ratio estimates. Geophysical Journal International, p. ggt130.
[73] Ghofrani, H., and G. M. Atkinson (2014). Site condition evaluation using horizontal-to-vertical response spectral ratios of earthquakes in the NGA-West 2 and Japanese databases, Soil Dynamics and Earthquake Engineering, 67, 30-43.
[74] Albarello, D., E. Lunedei (2011). Structure of an ambient vibration wavefield in the frequency range of emgineering interest ([0-5, 20] Hz): insights from numerical modelling, Near Surface Geophys. 9, 543-559.

[75] Oubaiche, EH, J-L Chatelain, A Bouguern, et al. (2012). Experimental Relationship Between Ambient Vibration H/V Peak Amplitude and Shear-wave Velocity Contrast. SRL, 83(6), 1038–1046.
[76] Hunter, J A, Crow, H L, Brooks, et al. (2010a). Seismic Site Classification and Site Period Mapping in the Ottawa Area Using Geophysical Methods; Geological Survey of Canada, Open File 6273; 80 pages; 1 DVD, doi:10.4095/286323.
[77] Benjumea, B, Macau, A, Gabas, A, Bellmuntm F, Figueras, S, Cires, J. 2011. Integrated geophysical profiles and H/V microtremor measurements for subsoil characterization. Near Surface Geophysics, 9 (5), 413-425.
[78] Yañez, G, M Muñoz, V Flores-Aqueveque, A Bosch (2015). Gravity derived depth to basement in Santiago Basin, Chile: implications for its geological evolution, hydrogeology, low enthalpy geothermal, soil characterization and geo-hazards, Andean Geology, 42, 190-212.
[79] Abuoelela A. Mohameda, A.M.A. Helalb, A.M.E et al. (2015). Effects of surface geology on the ground-motion at New Borg El-Arab City, Alexandria, Northern Egypt, doi:10.1016/j.nrjag.2015.11.005.
[80] Picozzi, M, A Strollo, S Parolai, E Durukal, O Özel, S Karabulut, J Zschau, and M Erdik (2009). Site characterization by seismic noise in Istanbul, Turkey. Soil Dynamics and Earthquake Engineering, 29(3), 469–482.
[81] Kamarudin, AH, ME Daud, Z Ibrahim, A Ibrahim (2016). Sustainable Non-destructive Technique Ambient Vibrations for Ground Assessments, Procedia – Social and Behavioral Sciences, 216, 701-711.
[82] Beroya, M.A.A., Aydin, A., Tilgo, R. & Lasala, M. (2009). Use of Microtremor in Liquefaction Hazard Mapping. Engineering Geology, 107, 140-153.
[83] Castellaro, S., R Panzeri, F Mesiti, L Bertello (2015). A surface seismic approach to liquefaction, SDEE, 77, 35-46.
[84] Michel C, Guéguen P, Lestuzzi P, Bard P-Y (2010) Comparison between seismic vulnerability models and experimental dynamic properties of existing buildings in France. Bull Earthq Eng 8(6):1295–1307.
[85] Oliveira CS, Navarro M (2010) Fundamental periods of vibration of RC buildings in Portugal from in situ experimental and numerical techniques. Bull Earthq Eng 8(3):609–642.
[86] Chiauzzi, L., Cassidy, J.F., et al. (2012). Estimate of the Fundamental Period of Reinforced Concrete Buildings: Code Provisions vs Experimental Measures in Victoria and Vancouver (BC, Canada). Proceedings 15WCEE, Paper 3033.
[87] Guillier B, Chatelain J-L, Tavera H, Perfettini H, Ochoa A, Herrera B (2014) Establishing empirical period formula for RC buildings in Lima, Peru: evidence for the impact of both the 1974 Lima earthquake and the application of the Peruvian seismic code on high-rise buildings., SRL 85,1308–1315.
[88] Salameh, C., B. Guillier, J. Harb, C. Cornou, P.-Y. Bard, C. Voisin, A. Mariscal (2016). Seismic response of Beirut (Lebanon) buildings: Instrumental results from ambient vibrations, Bull. Earthquake Eng., 10.1007/s10518-016-9920-9.
[89] Gorstein, M., & Ezersky, M. (2015). Combination of HVSR and MASW Methods to Obtain Shear Wave Velocity Model of Subsurface in Israel, International Journal of Geohazards and Environment, 1(1): 20-41.
[90] Pastén, C., Sáez, M., Ruiz, S., Leyton, F., Salomón, J., and Poli, P. (2016). Deep characterization of the Santiago Basin using HVSR and cross-correlation of ambient seismic noise, Engineering Geology, 201, 57–66.
[91] Yong, A., Martin, A., Stokoe, K., and Diehl, J., (2013). ARRA-funded VS30 measurements using multi-technique approach at strong-motion stations in California and central-eastern United States: USGS Open-File Report 2013–1102.
[92] Konno, K. & Ohmachi, T. (1998). Ground-motion characteristics estimated from spectral ratio between horizontal and vertical components of microtremor. Bull. Seism. Soc. Am., 88 (1), 228–241.
[93] Chiou, B., Darragh, R., Gregor, N., and Silva, W., 2008, NGA project strong-motion database: Eq. Spectra, 24, 23–44.
[94] Seyhan, E., Stewart, J.P., Ancheta, T.D., et al. (2014). NGA-West 2 Site Database: Earthquake Spectra, 30, 1007–1024.
[95] Hunter, JA, Burns RA, Good RL, Pullan SE, Pugin AJM, and Crow H, (2010b). Near-surface geophysical techniques for geohazards investigations: Some Canadian examples; The Leading Edge, 29, 936-947, doi:10.1190/1.3480011.
[96] Crow, H.L., Hunter, J.A., Motazedian, D., 2011. Monofrequency Insitu damping measurements in Ottawa area soft soils; Journal of Soil Dynamics and Earthquake Engineering, 31, 1669-1677.
[97] Benjumea, B, Hunter, J A, Burns, R A, Good, R L, Pullan, S E. (2001). Use of high-resolution shear-wave-reflection methods for determining earthquake fundamental site period response near Alfred, Ontario. Geological Survey of Canada, Current Research (Online) no. 2001-D3, 15 p., doi:10.4095/212122.
[98] Aylsworth, J.M., Lawrence, D.E., Guertin, J., 2000. Did two massive earthquakes in the Holocene induce widespread landsliding and near-surface deformation in part of the Ottawa Valley, Canada?, Geology 28, 903–906.
[99] Benjumea, B, Hunter, J A, Aylsworth, JM, Pullan, S E. 2003. Application of high-resolution seismic techniques in the evaluation of earthquake site response, Ottawa Valley, Canada, Tectonophysics, 368, 193–209.
[100] Motazedian D, Hunter JA, Pugin, AJM, and Crow H. 2011a. Development of a Vs30 (NEHRP) map for the city of Ottawa, Ontario, Canada, Canadian Geotechnical Journal 48: 458–472.
[101] Joyner WB, RE Warrick & TE Fumal, 1981. The effect of Quaternary alluvium on strong ground motion in the Coyote Lake, California, earthquake of 1979, Bull. Seis. Soc. Am., 71, 1333-1349.
[102] Benjumea, B., Hunter, J.A., Pullan, S.E., et al. (2008). Vs30 and Fundamental Site Period Estimates in Soft Sediments of the Ottawa Valley from Near-Surface Geophysical Measurements, J. Env. Eng. Geoph. 13 p.
[103] Dobry, R., I. Oweis, and A. Urzua (1976). Simplified procedures for estimating the fundamental period of a soil profile, Bull. Seismol.Soc. Am. 66, 1293–321.
[104] Motazedian D, Khaheshi Banab K, Hunter JA, Sivathayalan S, Crow H, and Brooks, G. 2011b. Comparison of Site Periods Derived from Different Evaluation Methods; BSSA, 101, 2942–2954, doi: 10.1785/0120100344.
[105] Hadijan, AH. 2002. Fundamental period and mode shape of layered soil profiles, SDEE. 22, 885-891.
[106] Pugin AJM, Brewer K, Cartwright T, Pullan SE, Perret D, Crow HL, Hunter JA, 2013. Near surface S-wave seismic reflection profiling – new approaches and insights, First Break, EAGE, 31, 49 – 60, doi: 10.3997/1365-2397.2013005.

[107] Ibrahim, K., AEA Mohamed, IS Babiker, AHG Elmula (2015). Local Site effects evaluation for Atbara area using microtremor measurements, American J. Earth Sciences, 2, 134-141.

[108] Lévêque, J-L, A Maggi, A Souriau (2010). Seismological constraints on ice properties at Dome C, Antarctica, from horizontal to vertical spectral ratios, Antarctic Science, 22, 572-579.

[109] Garofalo, F, S Foti, F Hollender, et al. (2016). InterPACIFIC project: Comparison of invasive and non-invasive methods for seismic site characterization. Part I: Intra-comparison of surface-wave methods, SDEE, 82, 222-240.

[110] Garofalo, F, S Foti, F Hollender, et al. (2016). InterPACIFIC project, Part II: Inter-comparison between surface-wave and borehole methods, SDEE, 82, 241-254.